Contribution from the Laboratoire de Spectroscopie Electronique, Facultês Universitaires N.D. de la Paix, B-5000 Namur, Belgium

Electronic Structure of Titanium(III) and Titanium(IV) Halides Studied by Solid-Phase X-ray Photoelectron Spectroscopy

Christine Mousty-Desbuquoit, Joseph Riga, and Jacques J. Verbist*

Received November 8, 1985

High-resolution XPS data have been obtained for titanium(III) and titanium(IV) fluorides, chlorides and bromides, all in the solid state. They are interpreted in terms of electronic structure and electron dynamic properties and compared to the available gas-phase photoelectron spectra and theoretical calculations.

1. Introduction

The d^0 and d^1 systems are among the simplest and most fundamental transition-metal complexes. Also in practical applications, they are recognized as very important because of their role in catalytic processes, such as the Ziegler–Natta stereospecific polymerization.

The TiX_4 (X = halogen) compounds have been intensively investigated by gas-phase X-ray photoelectron spectroscopy (XPS-g), and in a previous paper,[1] we presented a study of the electronic structure of $TiCl_4$ in the solid state by this technique (XPS-s).

X-ray photoelectron spectroscopy has been developed to a very powerful method for chemical bond studies, as it addresses the electrons involved in bond formation as well as the atomic-like, nonbonding electrons, which act as local probes of the molecular and solid-state structures. We will analyze in this way the electronic properties of Ti^{x+} (x = 3,4) transition-metal cations under the influence of various chemical surroundings, offered in this family by three halide ions: F^-, Cl^-, and Br^-.

2. Experimental Section

2.1. Compounds. All titanium halides analyzed in this work are listed in Table I. They include titanium halides TiX_n (X = F, Cl, Br) for the oxidation states +4 and +3, in their different modifications when available. The chemical instabilities of TiI_4 and β-$TiCl_3$ has prevented so far their study by solid-state XPS. All compounds are commercial (except for $TiCl_3$ samples). Their physical properties are summarized in Table II.

2.2. Sample Handling. All the samples are very hygroscopic and must be handled under inert atmosphere in a glovebox. A liquid sample ($TiCl_4$) was vaporized in the sample handling chamber and condensed as a thin film on a gold-plated surface, preliminarily cooled down with liquid nitrogen (180 K) (method II; see table I). Powder samples were presented as pellets (method I) or, if possible, sublimed and condensed as a thin film (TiF_4, $TiBr_4$) (method III). In spite of the precautions used during sample handling, most spectra obtained from powder pellets show some contamination by oxygen peaks. When the samples were purified by thin-film methods (methods II and III), no impurities were detected in the 0–1000-eV binding energy range during repeated experiments, except a small and constant O 1s peak in some cases.

Table I. Titanium Halides Studied in the Present Work

compd	origin	bulk purity, %	phase transition under 1 atm, °C	introduction method[b]
TiF_4	ROC-RIC	99	284 (subl)	I
	Ventron	98		I, III
$TiCl_4$	ROC-RIC	99.95	−24.8 (melt)	II
$TiBr_4$	Ventron	86.6	39 (melt)	I, III
TiF_3	ROC-RIC	95	1200 (subl)	I
	Ventron	98.5	930 (vacuum subl)	I
	Cerac	99		I, III
α-$TiCl_3$, γ-$TiCl_3$, δ-$TiCl_3$	Stauffer[a]		440 (dec)	I

[a] Samples supplied by the Specialty Chemicals Division, Stauffer Chemical Co. [b] Introduction methods: (I) powder pellets handled in a glovebox; (II) Vaporized and Condensed as a thin Film; (III) sublimed and condensed as a thin film.

2.3. X-ray Photoelectron Spectra. The XPS-s spectra have been recorded on a Hewlett-Packard 5950 A spectrometer using monochromatized Al Kα radiation ($h\nu$ = 1486.6 eV). TiF_4, $TiCl_4$, and $TiBr_4$ prepared as thin films were cooled down at respectively 273, 180, and 200 K during the analysis. The charging effects were controlled by a low-energy electron "flood gun".

3. Results

X-ray photoelectron spectra are presented in Figures 1–4. Peak positions, line widths, and areas were obtained by a weighted least-squares fitting of a model curve (50% Gaussian, 50% Lorentzian) to the experimental data using the Simplex method to minimize χ^2.[7]

In $TiCl_3$ samples, the oxide contamination is quite important and we have subtracted the unwanted TiO_2 contribution from Ti 2p and valence band spectra.[8] Whenever possible, the resulting Ti/Cl intensity ratio was checked for confirmation. These data handlings reveal the characteristic satellite structures associated with Ti 2p peaks of these compounds (Figure 2).

The TiF_3 sample, known as stable in air, still shows surface oxygen, in spite of handling under drastic conditions. Its surface purity is estimated at 85%, instead of the 99% bulk purity.

Calibration of spectra (i.e. defining the binding energy zero) is very difficult for this type of sample. The common technique of gold decoration could be used only in the case of α-$TiCl_3$ and TiF_4 pellets. For $TiCl_4$ films, the Cl $2p_{3/2}$ binding energy was set at 198.0 eV, the same value as found in α-$TiCl_3$.[1] In all three cases, the binding energy of the minor O 1s contamination peak coincides with that of TiO_2 (E_b (O 1s) = 530.3 ± 0.2 eV).[8]

All other samples have therefore been calibrated by setting the contamination O 1s peak binding energy at 530.3 eV. Results are collected in Tables III and IV. Even though no absolute binding energy values will be used in the following discussion, these numbers may prove useful for different purposes, such as comparison with other halides, e.g. a discussion on extramolecular

(1) Mousty-Desbuquoit, C.; Riga, J.; Verbist, J. J. *J. Chem. Phys.* **1983**, *79* 26.
(2) Alênoard, S.; Champetier, G. *C. R. Seances Acad. Sci., Ser. C* **1965**, *260*, 1977.
(3) (a) Brand, P.; Sackmann, H. *Z. Anorg. Allg. Chem.* **1963**, *321*, 262. (b) Berthold, H. J. *Angew. Chem.* **1974**, *13*, 575. (c) Höpke, R. Ph.D. Thesis, University of Hanover, FRG, 1969.
(4) (a) Brand, P.; Schmidt, J. *Z. Anorg. Allg. Chem.* **1966**, *348*, 257. (b) Rolsten, R. F.; Sisler, H. H. *J. Am. Chem. Soc.* **1957**, *79*, 5891. (c) Berthold, H. J., private communication.
(5) (a) Siegel, S. *Acta Crystallogr.* **1956**, *9*, 684. (b) Ehrlich, P.; Pietzka, T. *Z. Anorg. Allg. Chem.* **1954**, *275*, 121.
(6) (a) Natta, G.; Corradini, P.; Allegra, T. *J. Polym. Sci.* **1961**, *51*, 399. (b) Klem, W.; Krose, E. *Z. Anorg. Allg. Chem.* **1947**, *253*, 218. (c) Allegra, T.; Bassi, I. W. *Gazz. Chim. Ital.* **1980**, *110*, 437. (d) Guidetti, T.; Zannetti, R.; Ajo, D.; Marigo, A.; Vidali, M. *Eur. Polym. J.* **1980**, *16*, 1007. (e) Vlaic, T.; Bart, J. C. J.; Cavigiolo, W.; Mobilio, S.; Navarra, T. *Chem. Phys.* **1982**, *64*, 115. (f) Reed, J. W.; McWood, T. E. Presented at the National Meeting of the American Chemical Society, San Francisco, CA, 1958. Reed, J. W. *Diss. Abstr.* **1957**, *17*, 1479. (g) Cras, J. A. *Nature (London)* **1962**, *194*, 678.
(7) Thiry, P. A.; Ghijsen, J. Presented at the Annual Meeting of the Belgian Physical Society, 1980.
(8) Sen, S. K.; Riga, J.; Verbist, J. J. *Chem. Phys. Lett.* **1976**, *39*, 560; unpublished results.

0020-1669/87/1326-1212$01.50/0

Table II. Solid-State Structural Data and Physical Properties of Titanium Halides under Study

compd	color phase transition (under 1 atm)	cryst struct	Ti coordination no.	interatomic dist,[a] Å		
				atoms	intramolecular	intermolecular
TiF_4	white	cubic[2]	6	*b*		
$TiCl_4$	colorless	monoclinic[3]	4	Ti–Cl	2.18; 2.24	
				Cl–Cl	3.53; 3.68	3.67; 3.76
				Ti–Ti		5.05 (shortest)
$TiBr_4$	yellow orange	monoclinic[4]	4	Ti–Br	2.31; 2.43	
				Br–Br	3.71; 3.93	3.93; 3.96
				Ti–Ti		5.35 (shortest)
TiF_3	blue	rhombohedral[5]	6	Ti–F	1.97 (av)	ionic solid
α-$TiCl_3$	purple	hexagonal[6]	6	Ti–Cl	2.46	
				Ti–Ti	3.54	
β-$TiCl_3$	brown	ref 11	6	Ti–Cl	2.46	ionic solid
				Ti–Ti	2.91	
γ-$TiCl_3$	purple	ref 11	6	*c*		
δ-$TiCl_3$	purple	mixed cubic–hexagonal	6	*c*		

[a] Solid states. [b] Not well determined. [c] See α-$TiCl_3$.

Table III. Solid-State XPS Binding Energies (±0.2 eV) of Titanium Tetrahalides (eV)[a]

levels	energies		
	TiF_4	$TiCl_4$	$TiBr_4$
Ti $2p_{1/2}$	466.9	464.4	464.8
Ti $2p_{3/2}$	461.6	458.3	458.7
X(core)	F 1s 684.9	Cl $2p_{1/2}$ 199.5 Cl $2p_{3/2}$ 198.0	Br $3p_{1/2}$ 189.1 Br $3p_{3/2}$ 182.3
Ti 3p	39.8	37.3	37.7
X(valence)	F 2s 29.7	Cl 3s (IV) (17.3) Cl 3s (III) (15.9)	Br 4s 16.3
Ti–X (III)	10.2	6.0	5.8
X lone pairs (II)	8.0	4.2	4.2

[a] For labels, see Figure 1.

Table IV. Solid-State XPS Binding Energies (±0.2 eV) of Titanium Halides (eV)[a]

levels	energies			
	TiF_3	α-$TiCl_3$	γ-$TiCl_3$	δ-$TiCl_3$
Ti $2p_{1/2}$	465.5	463.6	463.0	463.4
Ti $2p_{3/2}$	459.9	457.6	457.0	457.6
X(core)	F 1s 684.9	Cl $2p_{1/2}$ 199.5 Cl $2p_{3/2}$ 198.0	199.5 198.0	199.5 198.0
Al 2p			74.5	74.6
Ti 3p	38.1	35.9	35.1	36.2
X(valence)	F 2s 30.0	Cl 3s 16.1	15.5	15.6
Ti–X (III)	9.2	6.0	5.9	5.9
Ti–X (II)	7.3	4.2	4.1	4.2
Ti 3d (I)	2.2	1.3	1.3	1.2

[a] For labels, see Figure 2.

relaxation in molecular solids that will be published later.[9]

4. Discussion

4.1. Titanium Core Levels. There are basically two ways in which core photoelectron peaks convey the information about the chemical surroundings of their origin.

The first way uses the exact value of the binding energy, which in turn depends on two factors: permanent effects, related to the nature and number of neighbors and bonding geometry; dynamic effects, due to the perturbation of the system by the photoemission process.

Second, we will discuss the detailed structure of the core peaks, revealing the existence of multiple final states upon photoemission. These satellites are quite interesting with respect to the valence electronic structure and properties.

(a) Chemical Shift. The spectra of Ti 2p core levels are shown in Figures 1 and 2; binding energies are given in Tables III and IV.

In many series of compounds, simple correlations have been found between core level shifts and chemically significant values, such as effective atomic charges.

In the present case, it will be noted that the Ti 2p levels systematically appear at higher binding energies for the tetrahalides than for the corresponding trihalide. Within each series, the higher E_b is found for the fluoride. These observations reflect the usual trend indicating a more positively charged Ti ion. However, it is difficult, because of the various calibrations techniques that had to be used for different compounds, to attempt a quantitative interpretation, which would rely on precise but perhaps inaccurate experimental data.

We will therefore rather concentrate our discussion on quantities that are not affected by such uncertainties, such as binding energy differences, or comparisons within well-defined subsets of samples. Full tables are only provided, with this warning, for clarity and convenience.

(b) Ti Core Levels in γ-$TiCl_3$. For $TiCl_3$, neither core nor valence levels data show any differences between the three crystallographic species, except for the lower binding energies of Ti 2p and Ti 3p peaks in γ-$TiCl_3$. The α and γ forms differ from one another in the close packing of their chlorides (hexagonal for α and cubic for γ) but differ also in the presence of Al^{3+} in γ-$TiCl_3$. Moreover, in δ-$TiCl_3$, also containing aluminium but where the Al 2p/Ti 2p relative intensity is only two-thirds of that in γ-$TiCl_3$, the binding energies are similar to those measured in α-$TiCl_3$. It seems thus that the chemical shift is related to the presence of Al^{3+} in solid γ-$TiCl_3$.

As the cation electronegativities of Ti^{3+} and Al^{3+} are quite similar,[10] this observation cannot be explained only by polarity considerations. Differences in polarizability, affecting the response of all other electrons to the creation of the photohole, are probably the reason for the higher kinetic energy (i.e. lower E_b) for the Ti 2p photoelectrons leaving the Al^{3+}-richer solids. Such an interpretation though should be confirmed by comparison with XPS data for γ-$TiCl_3$, synthesized without $AlCl_3$ cocrystallization.[11]

(c) Multiplet Splitting. The $3d^1$ compounds like TiF_3 and $TiCl_3$ can show multiplet structure in titanium core levels, while this is not the case for TiX_4 compounds. The structure arises when, upon photoionization of a core electron, the angular momenta of the resulting partially filled core shell couple with the angular momenta of various states of the atom before photoionization (unpaired valence electron angular momentum). Generally, the effect of multiplet splitting will be to produce[12] (1) asymmetry in the $2p_{3/2}$ peak toward the higher binding energy and in the $2p_{1/2}$ peak toward the lower binding energy, (2) enhancement of $2p_{1/2} - 2p_{3/2}$ splitting, and (3) a substantial area between the two main peaks remaining in the spectra after background subtraction.

(9) Mousty-Desbuquoit, C.; Riga, J.; Verbist, J. J., to be submitted for publication.

(10) Zhang, Y. *Inorg. Chem.* **1982**, *21*, 399.

(11) Boor, J., Jr. *Ziegler-Natta Catalysts and Polymerization*: Academic: New York, 1979.

(12) Sen, S. K. *Ann. Soc. Sci. Bruxelles, Ser. I* **1976**, *90*, 125.

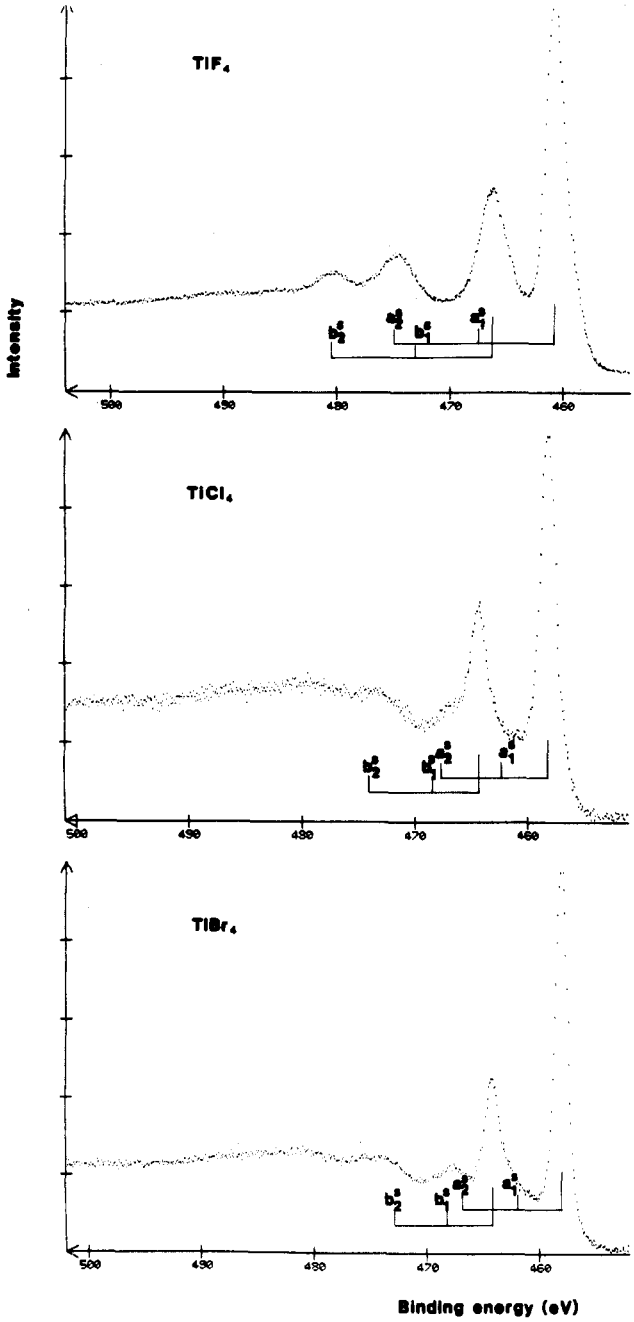

Figure 1. XPS Ti 2p core level spectra of titanium(IV) fluoride, chloride, and bromide.

The calculation of multiplet structure arising from the interaction of d electrons with a p hole in both the 2p and 3p shell of the titanium cation has been made by Yamaguchi et al.[13] This effect will be stronger on Ti 3p levels. The authors calculated the spectra of the 3p XPS peak of Ti^{3+} compounds with two or three components. The Ti 2p peak only shows a broadening.

Experimentally, no modification of the splitting between Ti 2p main peaks in Ti^{3+} ($3d^1$) has been observed with respect to that of Ti^{4+} ($3d^0$). We note however that the line widths of Ti 2p peaks increase by 0.8 eV in trihalides and that the Ti 3p peak is unresolved, with a high binding energy tail, which might simply be explained by the increase of the background.

(d) Shake-Up Satellites. These structures occur at higher binding energies than that of the main peak as the result of valence electron excitations simultaneous with core level photoemission.

Intense satellites have been observed in the gas-phase core photoemission spectra of Ti(IV) compounds.[14] These data can now be completed and compared to solid-state shake-up data (Table V).

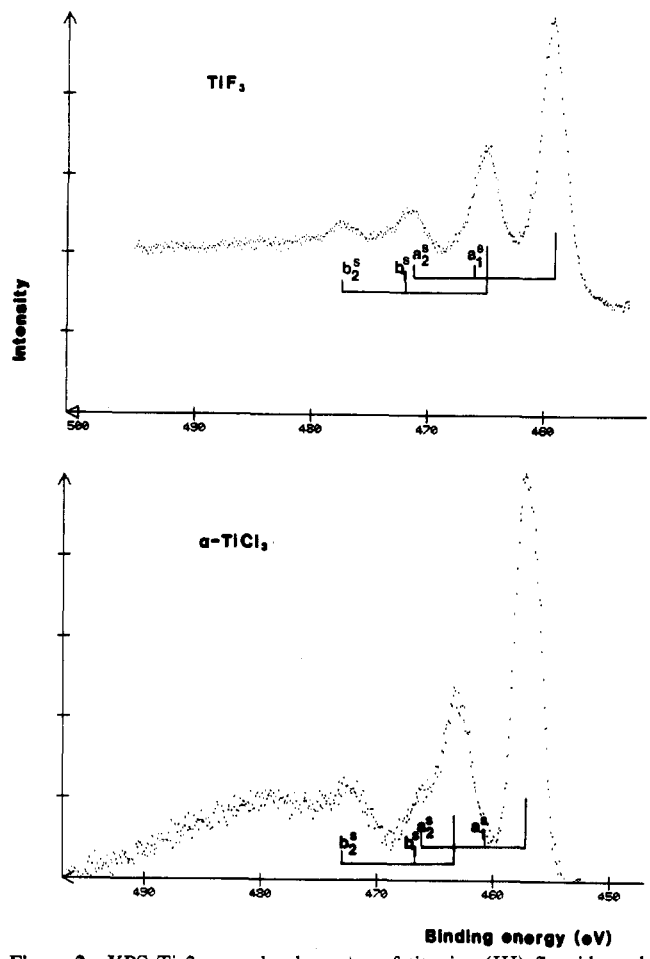

Figure 2. XPS Ti 2p core level spectra of titanium(III) fluoride and chloride.

To decipher the spectra (satellite positions and intensities) we used the approach described in ref 1. Also symbols are used in a similar manner (see Table V and Figures 1 and 2).

If one examines the Ti $2p_{1/2}$ component for $TiBr_4$ (Figure 1), the low binding energy side clearly presents a shoulder, indicating a satellite structure noted a_1^s. If one looks next at the Ti 2p doublet of TiF_4, the left-hand slope of the $^1/_2$ term shows a lower slope than the $^3/_2$ one, contrary to the Ti 2p main peaks in the other compounds. This can be explained by the presence of an underlying satellite, again a_1^s. Finally, there is no reason to ignore the existence of the same satellite, corresponding to its always observed b_1^s equivalent, in the case of $TiCl_4$.

The a_2^s and b_2^s peaks, with stronger intensities, are obvious for all three compounds. The weaker b_1^s are generally unresolved from a_2^s, but cannot be ignored from the shape of the latter, as confirmed by mathematical curve analysis.

Precise positions and intensities of all other satellites were obtained by a weighted least-squares fitting of model curves (50% Gaussian, 50% Lorentzian) to the experimental data using the Simplex method to minimize χ^2.

Besides these well-resolved satellites, there is a broader peak at higher relative binding energies, whose precise characteristics are difficult to define because of the background shape in this region of the spectrum. In all studied halides, its separation from the main peak is about 22–25 eV. These structures are interpreted

(13) Yamaguchi, T.; Mirva, Y. *J. Phys. Soc. Jpn.* **1972**, *45*, 200.

(14) Wallbank, B.; Perera, J. S. H. Q.; Frost, D. C.; McDowell, C. A. *J. Chem. Phys.* **1978**, *69*, 5405.

(15) Carlson, T. A.; Carver, J. C.; Saethre, L. J.; Garcia Santibanez, F.; Vernon, G. A. *J. Electron Spectrosc. Relat. Phenom.* **1974**, *5*, 247.

(16) Wallbank, B.; Johnson, C. E.; Main I. G. *J. Phys.* (*Les Ulis, Fr.*) **1973**, *C6*, L340.

Table V. Summary of Ti 2p Shake-Up Satellites in Solid- and Gas-Phase XPS: Labels, Separation Energies ΔE (eV), and Intensity Ratios (I/I_0)

compd	satellite		XPS-s[a] Ti $2p_{1/2}$	XPS-s[a] Ti $2p_{3/2}$	XPS-s[b] Ti $2p_{1/2}$	XPS-s[b] Ti $2p_{3/2}$	XPS-g[c] Ti $2p_{1/2}$	XPS-g[c] Ti $2p_{3/2}$	ref for XPS-s
TiF_4	b_1	a_1	6.6 (0.16)[d]	6.6 (0.16)			...	7.1 (0.12)	15
	b_2	a_2	14.1 (0.26)	14.1 (0.30)		14.7 (0.11)	13.9 (0.43)	13.0 (0.19)	15
$TiCl_4$	b_1	a_1	4.0 (0.12)[d]	4.0 (0.12)			...	4.0 (0.14)	
	b_2	a_2	9.7 (0.28)	9.4 (0.08)			9.8 (0.41)	9.4 (0.16)	
$TiBr_4$	b_1	a_1	3.8 (0.08)[d]	3.8 (0.08)			...	3.3 (0.06)	
	b_2	a_2	8.5 (0.17)	8.7 (0.10)			8.9 (0.40)	8.5 (0.14)	
TiI_4	b_1	a_1					...	2.1 (0.06)	
	b_2	a_2					7.3 (0.25)	7.2 (0.18)	
TiF_3	b_1	a_1	7.0 (0.06)[d]	7.0 (0.06)					
	b_2	a_2	12.2 (0.36)	12.3 (0.22)	12.7	12.4			16
		a_2				13.0 (0.11)			15
$TiCl_3$	b_1	a_1	3.3 (0.02)[d]	3.3 (0.02)					
	b_2	a_2	9.6 (0.40)	9.0 (0.09)					
TiO_2	b_1	a_1			5.0 (0.07)	5.1 (0.07)			8
	b_2	a_2			13.3 (0.40)	13.5 (0.25)			

[a] This work. [b] Literature values. [c] Reference 14. [d] Fixed values.

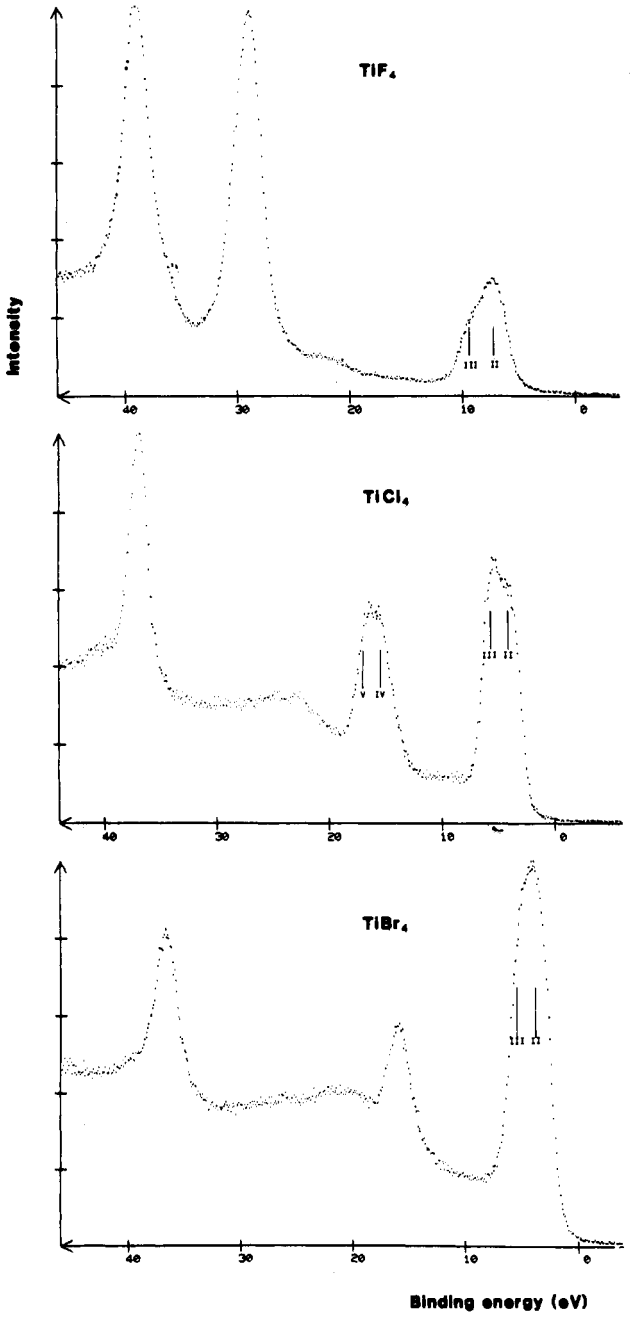

Figure 3. XPS valence band spectra of titanium(IV) fluoride, chloride, and bromide.

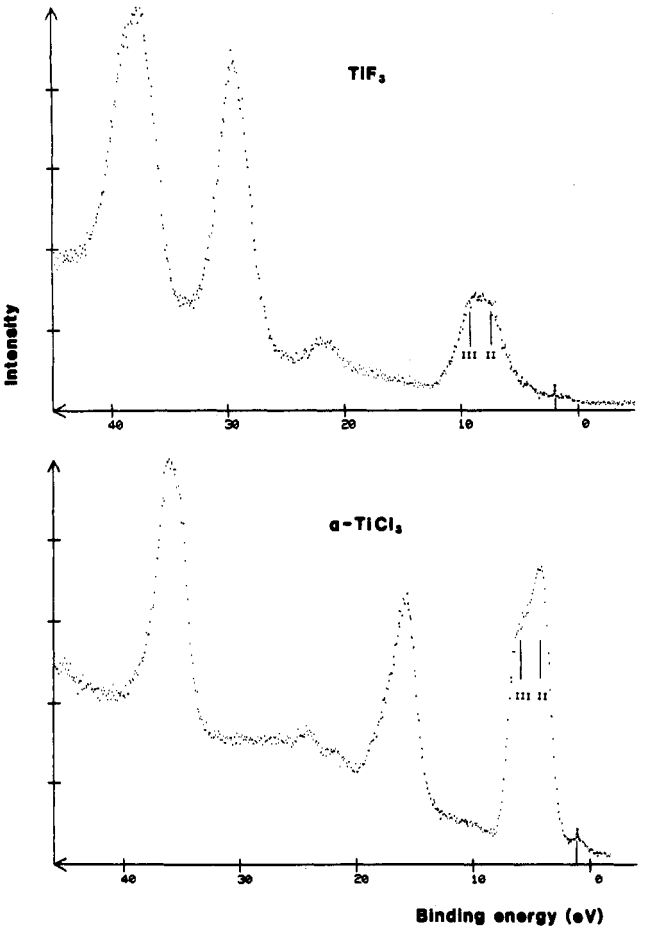

Figure 4. XPS valence band spectra of titanium(III) fluoride and chloride.

as inelastic energy loss peaks. Similar features are observed in the halogen core levels.[1]

Several observations can be made from the data in Table V: there are *two* satellites associated with each main peak, a low-energy satellite ($\Delta E_1 \sim 2$–8 eV), a high-energy satellite ($\Delta E_2 \sim 10$ eV); the satellite to main peak separation (ΔE) *increases* with the electronegativity of the ligand; the relative intensity (I/I_0) simultaneously *increases*; the intensity of the second satellite (b_2) is generally higher than that of the first one (b_1); comparison of the TiF_4 in gas (tetrahedral) and solid (octahedral) coordinations shows that satellite separation and intensity are sensitive to changes in site.

These satellite lines observed in core level XPS spectra of molecules have been interpreted in terms of single-valence-electron

Table VI. UV Absorption Charge-Transfer Energies vs. Low-Energy Satellite Energies Separations (ΔE_{a_1}) (eV)

compd	ΔE_{a_1}	ΔE(L *np* → 3d)	ref
$TiCl_4$	4.0	4.4–5.3	32
$TiBr_4$	3.3	3.6–4.5	32
TiI_4	2.1	2.4–3.3	32
TiF_3	7.0	6.2	33
α-$TiCl_3$	3.3	2.3	34

Table VII. Comparison of Theoretical and Experimental Ti $2p_{3/2}$ Shake-Up Satellites (eV)

		calcd			exptl	
compd	transition	ΔE	I/I_0	ref	ΔE_{a_1}	I/I_0
TiF_4 (TiF_6^{2-})	$t_{2g} \rightarrow t_{2g}^*$	4.7	0.12	23	6.6	0.16
	$e_g \rightarrow e_g^*$	7.6	0.11			
$TiCl_4$	$1e \rightarrow 2e$	3.0	0.1168	27		
	$2t_2 \rightarrow 4t_2$	4.6	0.0852			
	$1e \rightarrow 2e$	2.77	0.03	29	4.0	0.12
	$3t_2 \rightarrow 4t_2$	3.40	0.0026			
	$2t_2 \rightarrow 4t_2$	4.12	0.0738			
TiF_3 (TiF_6^{3-})	$t_{2g} \rightarrow t_{2g}^*$ [a]	6.8		33a		
	$e_g \rightarrow e_g^*$	12.6				
	$t_{2g} \rightarrow t_{2g}^*$	7.05		33b	7.0	0.06
	$e_g \rightarrow e_g^*$	8.99				
α-$TiCl_3$ ($TiCl_6^{3-}$)	$t_{2g} \rightarrow t_{2g}^*$ [a]	4.16		33b	3.3	0.02
	$e_g \rightarrow e_g^*$	5.63				

[a] Calculations performed on TiF_6^{3-} and $TiCl_6^{3-}$ Clusters without considering relaxation effects.[42]

excitations obeying the monopole selection rule.[17] The two outer orbitals involved in this process should thus have the same symmetry, whatever their nature. A considerable controversy has risen regarding the interpretation of these satellites.[18-31]

The most generally accepted hypothesis involves a ligand (L *np*) to metal (3d) charge-transfer process.[21] This type of assignment has previously been made on the basis of comparison with UV absorption spectra, but the different selection rules should not be overlooked and constitute a limiting factor.[28] As examples, in table VI, the optical absorption energies are compared with photoemission low-energy satellite energies of the TiX_n compounds.[32-34] Within this class of compounds, UV absorption ($1t_1 \rightarrow 2e$) ($1t_1 \rightarrow 3t_2$) energies may give a qualitative idea of the expected first satellite positions.[30] Energies and intensities of ligand to metal shake-up transitions may be calculated with reasonable accuracy by using the SCF-Xα method.[23,27,29,30] In this case, theoretical methods, UV absorption energies and low-energy

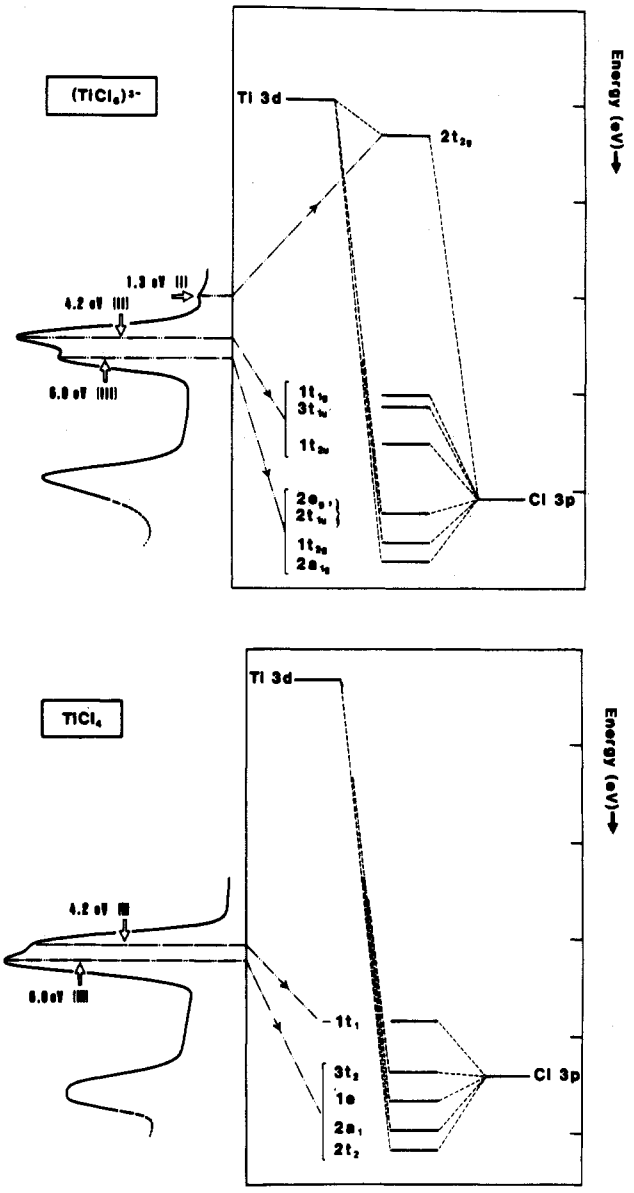

Figure 5. Comparison of the XPS valence band spectra of $TiCl_3$ and $TiCl_4$.

satellite energies are in good agreement, indicating that these satellites (a_1, b_1) arise from ligand to metal charge-transfer excitations ($t_{2g} \rightarrow t_{2g}^*$, $e_g \rightarrow e_g^*$), unresolved in the XPS spectra. If the low-energy satellite (a_1, b_1) can be explained in this way, the nature of the intense one at high energy (a_2, b_2) cannot be accounted for by this model. As alternative mechanism, we could suggest that these are due to ligand to metal conduction band transitions (e.g. 4s and 4p orbitals).[22,26,27,30] Theoretical values of ligand to metal 4s, 4p transition energies agree well with our experimental observations (Table VII). However, the calculated intensities are very small, opposing an adverse argument to this interpretation.

Recently, a new account of this model has been proposed by Gupta and Tossell[30] and de Boer et al.[31] They suggest that the high-energy photoelectron satellite may correspond to a shake-off transition to a structured part of the continuum[30] or, in other words, to an exciton (virtual bound state).[31] This formulation is very similar to so-called "shape-resonance" resulting from trapping of low-energy electrons in the potential arising from the cage of electronegative ligand.[35] Similar features have been observed by X-ray absorption near-edge structures (XANES) at

(17) Fadley, C. S. *Electron Emission Spectroscopy*; Dekeyser, W., Fiermans, L., Vanderkelen, G., Vennik, J., Eds.; D. Reidel: Dordrecht, The Netherlands, 1973.
(18) Wendin, G. *Struct. Bonding* (Berlin) **1981**, *45*, 1.
(19) Rosencwaig, A.; Wertheim, G. K.; Guggenheim, H. J. *Phys. Rev. Lett.* **1971**, *27* 479.
(20) Yin, L.; Adler, I.; Tsang, T.; Matienzo, L. J.; Grim, S. O. *Chem. Phys. Lett.* **1974**, *24*, 81.
(21) Kim, K. S. *J. Electron Spectrosc. Relat. Phenom.* **1974**, *3*, 217.
(22) Ikemoto, I.; Ishii, K.; Kuroda, H.; Thomas, J. M. *Chem. Phys. Lett.* **1974**, *28*, 55.
(23) Larsson, S. *J. Electron Spectrosc. Relat. Phenom.* **1976**, *8*, 171.
(24) Larsson, S. *Chem. Phys. Lett.* **1976**, *40*, 362.
(25) Asada, S.; Sugano, S. *J. Phys. Soc. Jpn.* **1976**, *41*, 1291.
(26) Tossell, J. A. *J. Electron Spectrosc. Relat. Phenom.* **1976**, *8*, 1.
(27) Tossell, J. A. *Chem. Phys. Lett.* **1979**, *65*, 371.
(28) Robert, T. Ph.D. Thesis, University of Mons, Mons, Belgium, 1980, and references therein.
(29) Tse, J. S. *Chem. Phys. Lett.* **1981**, *77*, 373.
(30) Gupta, A.; Tossell, J. A. *J. Electron Spectrosc. Relat. Phenom.* **1982**, *26*, 223.
(31) de Boer, D. K. G.; Haas, C.; Sawatzky, C. A. *Phys. Rev B: Condens. Matter* **1984**, *29*, 4401.
(32) Di Sipio, L.; Michelis, G. D.; Tondello, E.; Oleari, L. *Gazz. Chem. Ital.* **1966**, *96*, 1785.
(33) (a) Bedon, H. D.; Horner, S. M.; Tyree, S. Y. *Inorg. Chem.* **1964**, *3*, 647. (b) Rösch, N.; Johnson, K. H. *J. Mol. Catal.* **1975/1976**, *1*, 395.
(34) Clark, R. J. H. *J. Chem. Soc.* **1964**, 417.
(35) Dehmer, J. L. *J. Chem. Phys.* **1972**, *56*, 4496. Dehmer, J. L.; Dill, D. *J. Chem. Phys.* **1976**, *65*, 53.

the FeK edge of $K_3Fe(CN)_6$ and $K_4Fe(CN)_6$ and interpreted by means of multiple scattering calculations.[36] A comparative analysis of XPS, XANES results, and multiple scattering calculations realized on titanium halide compounds would probably confirm this bound-state formulation.

In summary, it is found that core level shake-up satellites are quite sensitive to chemical bonding, by both their relative position and their intensity.

Their separation from the main peak, corresponding to a valence electron excitation, correlates rather well with the existing data from UV absorption spectroscopy and theoretical calculations. The present consistent set of XPS data extends over compounds for which no other data are presently available.

The effect of metal oxidation state can be observed by comparing TiF_4 and TiF_3. The metal ion being octahedrally coordinated in both, the splitting is larger for the lower oxidation state, reflecting the expected shift of the parent level to lower energy. This effect however is dominated by that of coordination geometry; from $TiCl_4$ (tetrahedral) to $TiCl_3$ (octahedral) the splitting decreases, as it does from gaseous (tetrahedral) to solid (octahedral) TiF_4 (considering the first satellite only because of the different analysis of the second one in the gas-phase literature data).

The relative intensity evolution should be taken with care, due to the different origin of the first two (and major) satellites. However, in both cases, the increase with ligand electronegativity and with metal oxidation state supply experimental evidence for the primarily dynamic character of the shake-up phenomena: their probability is enhanced by the relative increase in covalent character of the bond upon photoemission.

4.2. Valence Levels. The valence band spectra (recorded from 0 to 50 eV) are presented in Figures 3 and 4. They show on one side, inner valence peaks with essentially atomic character (Ti 3p, F 2s or Cl 3s or Br 4s) and a band located between 10 and 4 eV, constituted by electronic levels of the Ti–X bond (X *np*–Ti 3d, 4s bonding). The poorly resolved structure around 23 eV is related to the growth of oxygen contamination during long accumulation (O 2s). The valence band can be resolved in two (II, III) (TiX_4) or three (I, II, III) components (TiX_3). The binding energies of all these peaks are listed in Tables III and IV. The bonding band intensity, relative to Ti 3p, reflects the cross-section of the dominant halogen character.

In the case of tetrahedral TiX_4 compounds, and by comparison with the UPS data,[37-41] component II in Figure 5 is identified with the nonbonding lone pairs of halogens ($1t_1^6$ (π)), and the other four orbitals, $2t_2^6$, $2a_1^2$, $1e^4$, and $3t_2^6$, as unresolved in component III. Indeed, the separation between peaks II and III on the XPS spectra is nearly identical with that measured in UPS between the line of the lone-pair orbital ($1t_1$) and the mean value of the binding energies of the other four orbitals.[40]

In the $TiCl_4$ valence band spectrum, the Cl 3s peak shows the particular structure discussed in a former paper.[1] A theoretical investigation of this problem is in progress and the results, regarding the different possible interpretations, will be presented elsewhere.[42]

Trihalides have octahedrally coordinated Ti ions with one 3d unpaired electron situated in the $2t_{2g}$ orbital (peak I, Figure 4). When one compares $TiCl_3$ and $TiCl_4$ valence band spectra, it is interesting to note that peaks II and III have reversed intensities (Figure 5). The differences between these two compounds is that the former has a $3d^1$ electronic structure in octahedral coordination and the second is a $3d^0$ tetrahedral compound.

5. Conclusions

A detailed analysis of the X-ray photoelectron spectra, obtained in the solid state from titanium(III) and titanium(IV) halides, gives a clear and rather well-resolved picture of the electron distribution associated with the chemical bonding and of its dynamic properties upon photoemission.

Core and valence binding energies have been tabulated for compounds of which several are extremely difficult to handle in vacuum. The observed values, as well as the shake-up satellites of the core levels, convey information about the way in which the nature and number of ligands around the metal ion, and eventually the presence of Al^{3+} ions in the lattice, affect the screening of the Ti 2p photoholes by the outer electrons.

Acknowledgment. The authors are grateful to Dr K. B. Triplett (Stauffer Chemical Co., Dobbs Ferry, NY), who supplied several samples of $TiCl_3$, to Professor Dr H. J. Berthold (University of Hanover, FRG) for supplying crystallographic data on $TiBr_4$, and to Dr. H. Chermette (Université Claude Bernard, Lyon, France) for stimulating discussions. C.M.D. thanks IRSIA (Belgium) for a doctoral fellowship.

Registry No. TiF_4, 7783-63-3; $TiCl_4$, 7550-45-0; $TiBr_4$, 7789-68-6; TiF_3, 13470-08-1; $TiCl_3$, 7705-07-9; Ti, 7440-32-6; F_2, 7782-41-4; Cl_2, 7782-50-5.

(36) Bianconi, A.; Dell'Ariccia, M.; Durham, P. J.; Pendry, J. B. *Phys. Rev. B: Condens. Matter* **1982**, *26*, 6502.
(37) Cox, P. O.; Evans, S.; Hammett, A.; Orchard, A. F. *Chem. Phys.* **1970**, *7*, 414.
(38) Egdell, R. G.; Orchard, A. F.; Lloyd, D. R.; Richardson, N. V. *J. Electron Spectrosc. Relat. Phenom.* **1977**, *12*, 415.
(39) Green, J. C.; Green, M. L. H.; Joachim, P. J.; Orchard, A. F.; Turner, D. W. *Philos. Trans. R. Soc. London, A* **1970**, *268*, 111.
(40) Egdell, R. G.; Orchard, A. F. *J. Chem. Soc., Faraday Trans 2* **1978**, *74*, 485.
(41) Bancroft, G. M.; Pellach, E.; Tse, J. S. *Inorg. Chem.* **1982**, *21*, 2950.
(42) Chermette, H.; Mousty-Desbuquoit, C.; Goursot, A.; Pertosa, P.; Boutique, J. P.; Riga, J.; Verbist, J. J., submitted for publication in *Chem. Phys.*